function described in Appendix B. The general solution for the interior is given by

$$\psi_i(\mathbf{r}) = \sum_{n=0}^{\infty} B_n r^n P_n(\cos\theta) \qquad (A8)$$

where again the boundary conditions determine the coefficients B_n. The determination of the coefficients in eq A7 is facilitated by using a spherical expansion for the screened Coulomb potential. Taking the Fourier transform and using the plane wave expansion,[19] we get

$$\frac{\exp(-\kappa|\mathbf{r} - \mathbf{r}_0|)}{|\mathbf{r} - \mathbf{r}_0|} =$$

$$\frac{2}{\pi}\sum_{n=0}^{\infty}\int_0^{\infty}dk\,\frac{k^2}{k^2 + \kappa^2}j_n(kr)\,j_n(kr_0)(2n + 1)P_n(\cos\theta) \quad (A9)$$

with j_n a modified spherical Bessel function. The integral can be evaluated[19] and written in terms of two other modified spherical Bessel functions, namely

$$\frac{\exp(-\kappa|\mathbf{r} - \mathbf{r}_0|)}{|\mathbf{r} - \mathbf{r}_0|} = \sum_{n=0}^{\infty}(2n + 1)\kappa k_n(\kappa r_0)\,i_n(\kappa r)P_n(\cos\theta) \quad (A10)$$

where $r \le r_0$. The properties of $i_n(x)$ are also discussed in Appendix B. If we substitute this expression into (A7), using the boundary conditions (A3) and (A4) and the relations (B5) and (B6) in the following appendix, it is straightforward to derive eq 10.

Appendix B

The modified spherical Bessel functions used in this work are described in most elementary tables (see for example ref 19). For convenience, we list some of the relevant properties here. Explicit expressions for these functions are

$$i_n(x) = (1/2x)\{e^x A_n(x) + e^{-x} B_n(x)\} \qquad (B1)$$

with

$$A_n(x) = \sum_{k=0}^{n}\frac{(-1)^k(n + k)!}{k!\,(n - k)!\,(2x)^k} \qquad (B2)$$

$$B_n(x) = (-1)^{n+1}\sum_{k=0}^{n}\frac{(n + k)!}{(n - k)!\,(2x)^k} \qquad (B3)$$

and

$$k_n(x) = \frac{e^{-x}}{x}\sum_{k=0}^{n}\frac{(n + k)!}{k!\,(n - k)!\,(2x)^k} \qquad (B4)$$

Their derivatives satisfy the following relations

$$i_n'(x) = (n/x)i_n(x) + i_{n+1}(x) \qquad (B5)$$

and

$$k_n'(x) = (n/x)k_n(x) - k_{n+1}(x) \qquad (B6)$$

For the arguments used in this work, the explicit expressions were not able to be generated with sufficient precision as soon as n exceeded about 4. Thus, for larger n, we made use of the following recursion formulas and techniques described in ref 20

$$i_{n+1}(x) = i_{n-1}(x) - \frac{2n + 1}{x}i_n(x) \qquad (B7)$$

$$k_{n+1}(x) = k_{n-1}(x) + \frac{2n + 1}{x}k_n(x) \qquad (B8)$$

Finally, we note that the modified spherical functions $\mathbf{k}_n(x)$, used by Head-Gordon and Brooks,[8,16] are related to those used here via

$$k_n(x) = \frac{(2n - 1)!!\,e^{-x}}{x^{n+1}}\mathbf{k}_n(x) \qquad (B9)$$

Substituting this expression into eq 8 gives precisely eq A9 of ref 8.

Registry No. Superoxide dismutase, 9054-89-1; superoxide, 11062-77-4.

Statistical Thermodynamics of Molecular Organization in the Inverse Hexagonal Phase

Linda Steenhuizen, Diego Kramer, and Avinoam Ben-Shaul*

Department of Physical Chemistry and The Fritz Haber Research Center for Molecular Dynamics, The Hebrew University, Jerusalem 91904, Israel (Received: January 28, 1991)

A mean field theory of chain packing in amphiphilic aggregates is used to calculate conformational and thermodynamic properties of the inverse hexagonal phase. These properties are compared with those for planar bilayers and curved monolayers. Calculated bond order parameters reveal that chains packed in the hexagonal arrangement have more conformational freedom than chains packed in a bilayer. The calculated order parameters are in good agreement with recent experimental results. Free energy calculations are also presented. It is found that for small areas per head group the packing free energy of amphiphiles in a bilayer is considerably higher than in the hexagonal phase.

1. Introduction

Aqueous solutions of amphiphilic molecules exhibit rich and complex phase behaviors.[1] Amphiphiles assemble in aggregates

of different structures, depending on their chemical nature as well as on temperature and concentration. At low concentrations the stable phases are usually isotropic solutions of micellar aggregates of various shapes (e.g., spherical, cylindrical, vesicles) and sizes. At higher concentrations the aggregates grow and organize in partially ordered (e.g., nematic) or fully ordered phases characterized by lamellar, hexagonal, or cubic symmetries.

(1) (a) Tiddy, G. J. T. *Phys. Rep.* **1980**, *57*, 1. (b) Wennerstrom, H.; Lindman, B. *Phys. Rep.* **1979**, *52*, 1. (c) Larson, R. G. *J. Chem. Phys.* **1989**, *91*, 2479. (d) Ekwall, P. *Adv. Liq. Cryst.* **1975**, *1*, 1.

(2) (a) Ben-Shaul, A.; Gelbart, W. M. *Annu. Rev. Phys. Chem.* **1985**, *86*, 179. (b) Gruen, D. W. R. *J. Phys. Chem.* **1985**, *89*, 146. (c) Dill, K. A.; Cantor, R. S. *Macromolecules* **1984**, *17*, 380. (d) Leemarkers, F. A. M.; Scheutjens, J. M. H. M.; Lyklema, J. *Biophys. Chem.* **1983**, *18*, 353. (e) Marcelja, S. *Biochim. Biophys. Acta* **1974**, *367*, 165.

(3) (a) Van der Ploeg, P.; Berendsen, H. J. C. *Mol. Phys.* **1983**, *49*, 233. (b) Egberts, E.; Berendsen, H. J. C. *J. Chem. Phys.* **1988**, *89*, 3718. (c) Watanabe, K.; Ferrario, M.; Klein, M. L. *J. Phys. Chem.* **1988**, *92*, 819.
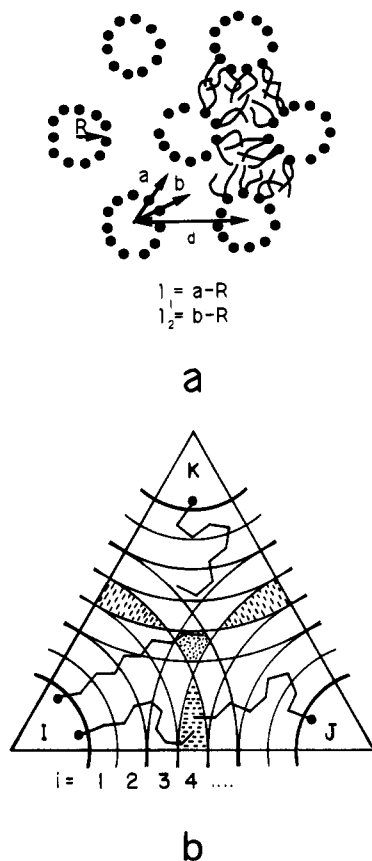
a

b

Figure 1. Schematic illustration of the H_{II} phase (a) and the division of the hydrophobic core into (hypothetical) layers (b). The dashed and dotted areas represent regions of two and three layers overlap, respectively.

Amphiphilic aggregates and phases can be classified as "regular" or "inverse". In a regular aggregate, the hydrophobic core is convex and the hydrophilic heads point out toward a continuous aqueous solution. In an inverse phase, the hydrophobic tails form a continuous medium while the hydrophilic heads point into convex aqueous regions. One example of the second class is the inverse hexagonal phase (H_{II}), schematically shown in Figure 1, where the water is confined to the interior of (infinitely long) parallel cylinders arranged in an hexagonal lattice.

Extensive literature is available concerning the thermodynamics and the microscopic structure of regular aggregates such as micelles of different shapes, or bilayers. For these aggregates, conformational properties, such as bond order parameters, or spatial distribution of chain segments, have been measured by various techniques[4,5] and calculated by use of different models.[2,3] On the other hand, relatively little is known about the inverse phases. Thus, in this paper we present a theoretical study, focusing on the inverse hexagonal phase, for which partial experimental information is available[5,6a] and the theoretical analyses are mostly qualitative.[6b] More specifically, in the following sections we shall analyze several conformational and thermodynamic properties of the H_{II} phase and compare them with those of the L_α phase. The L_α phase, as shown schematically in Figure 2, consists of a lamellar array of planar bilayers.

Our approach is based on the application of a recent mean field theory of chain-packing statistics and thermodynamics in amphiphilic aggregates.[2a,8] This theory has previously been suc-
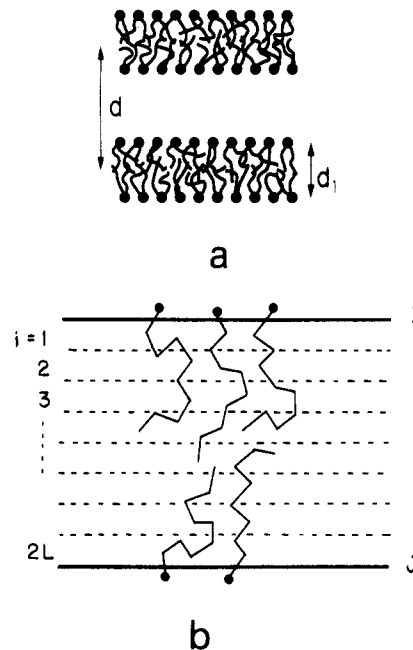

a

b

Figure 2. Schematic illustration of the L_α phase (a) and the division of the hydrophobic core into parallel layers (b).

cessfully applied to the calculation of chain conformational properties, such as bond order parameters along the hydrocarbon chain, segment spatial distributions, or the average fraction of gauche bonds.[10] It has also been used to calculate thermodynamic properties such as the packing free energies in different geometries[10b] and elastic moduli of bilayers and monolayers.[9]

In this paper, the theory will be employed to calculate C–D- (C–H) bond order parameters of amphiphile chains in the L_α and H_{II} phase and to compare them with experimental results obtained by Sternin et al.[5] using deuterium NMR spectrometry. We shall also present free energy calculations of the two phases in order to assess their relative stability.

2. Theory

(a) Singlet Probability Distribution. The central quantity in our analysis is the singlet probability distribution (spd), $P(\alpha|G)$. This is the probability that in a given geometry "G" the amphiphilic molecule will be found in conformation α. We consider single-chain amphiphiles of the form $H(CH_2)_{n-1}CH_3$, with H denoting the polar head group. We assume that the head group is structureless. Accordingly, the molecular conformation α is determined by the following: (i) the sequence of internal bond rotations (trans/gauche) along the hydrocarbon chain $(CH_2)_{n-1}CH_3$, (ii) the three Euler angles specifying the overall orientation of the chain relative to the hydrocarbon water interface, and (iii) the distance of the head group from the interface. (In the calculations, the head group is confined to a narrow interval around the interface; see section 3.)

The geometry G is specified by the curvature of the hydrocarbon–water interface (onto which the head groups are anchored) and by the area per head group, a, at the interface. For example, in the inverse hexagonal phase, the interface has a cylindrical geometry and the area per head group is a function of the cylinders' radii and the distance between them.

Formally the spd can be expressed as

$$P(\alpha|G) = (1/Z) \exp[-\beta W(\alpha|G)] \qquad (1)$$

(4) Seelig, J.; Niederberger, W. *Biochemistry* **1974**, *13*, 1585.

(5) Sternin, E.; Fine, B.; Bloom, M.; Tilcock, C. P. S.; Wong, K. F.; Cullis, P. R. *Biophys. J.* **1988**, *54*, 689.

(6) (a) Kirk, G. L.; Gruner, S. M. *J. Phys.* **1985**, *46*, 761. (b) Kirk, G. L.; Gruner, S. M.; Stein, L. *Biochemistry* **1984**, *23*, 1093.

(7) Reiss-Husson, F. *J. Mol. Biol.* **1967**, *25*, 367.

(8) Ben-Shaul, A.; Szleifer, I.; Gelbart, W. M. *J. Chem. Phys.* **1985**, *83*, 3597.

(9) Szleifer, I.; Kramer, D.; Ben-Shaul, A.; Roux, D.; Gelbart, W. M. *Phys. Rev. Lett.* **1988**, *60*, 1966.

(10) (a) Szleifer, I. Ph.D. Thesis, Hebrew University of Jerusalem, September 1988. (b) Szleifer, I.; Ben-Shaul, A.; Gelbart, W. M. *J. Chem. Phys.* **1987**, *86*, 7094.

(11) Cullis, P. R.; de Kruijff, B. *Biochim. Biophys. Acta* **1979**, *559*, 399.

(12) Tanford, C. *The Hydrophobic Effect*; Wiley: New York, 1980.

(13) Mitchell, D. J.; Ninham, B. W. *J. Chem. Soc., Faraday Trans. 2* **1988**, *77*, 601.

where W is a potential of mean force acting on a chain in conformation α, $Z = \sum_\alpha \exp[-\beta W(\alpha|G)]$ is the partition function, and $\beta = 1/kT$. To a first approximation W can be divided into two parts, corresponding to chain (tail) and head-group contributions, $W = W_c(\alpha) + W_h$. W_h accounts for the effects of interactions between the head group and (i) neighboring head groups, (ii) the solvent molecules, and (iii) the chains in the hydrophobic core. Assuming that W_h is independent of α corresponds to the assumption that the internal organization of the chains in the core does not affect head-group interactions. The separation of head and tail contributions, $W = W_c(\alpha) + W_h$, implies a corresponding separation of the free energy per molecule

$$\beta A = -\ln Z = -\ln Z_c - \ln Z_h = \beta A_c + \beta A_h \qquad (2)$$

An exact calculation of W_h and hence A_h is very difficult. We shall need these quantities for comparing the relative stability of the H_{II} and L_α phases, to which end we shall use a familiar approximate phenomenological model. Note however that W_h does not affect our main goal, namely, the calculation of $P(\alpha|G)$.

Because of the extreme complexity of amphiphilic aggregates we cannot calculate $P(\alpha|G)$ exactly. Instead we derived $P(\alpha|G)$, and thus also the effective potential, by a mean field approach.[2a,8] Explicitly, we seek the probability distribution function which minimizes the free energy per chain A_c

$$A_c = E_c - TS_c = \sum_\alpha P(\alpha|G)\epsilon(\alpha) + kT\sum_\alpha P(\alpha|G)\ln P(\alpha|G) \qquad (3)$$

subject to the packing constraints on $P(\alpha|G)$ corresponding to the given aggregation geometry. The quantity $\epsilon(\alpha)$ is the internal chain energy. In the rotational isomeric state (RIS)[14] model it is given by $\epsilon(\alpha) = n_g(\alpha)\epsilon_g$, with $n_g(\alpha)$ denoting the number of gauche bonds in configuration α and ϵ_g denoting the gauche energy.

The packing constraints follow from the (single) assumption that the hydrophobic core is dry and uniformly packed with chain segments, at liquidlike density. The mathematical formulation of the constraints reflects the aggregation geometry. The geometry is conveniently characterized by dividing the hydrophobic core into L parallel (or concentric) layers of width Δl, as illustrated in Figures 1 and 2. Using M_i to denote the volume of layer i and N for the total number of chains that can reach this layer, then the average volume per chain in layer i is $m_i = M_i/N$. Now let $\phi_i(\alpha)$ denote the volume that a chain in conformation α occupies in layer i. The requirement for uniform density implies

$$\sum_\alpha P(\alpha)\phi_i(\alpha) = \langle\phi_i(\alpha)\rangle = m_i \qquad i = 1, ..., L \qquad (4)$$

which means that $\langle\phi_i(\alpha)\rangle$, the average volume occupied by a chain in layer i, is equal to the average volume available (per chain) in this layer, m_i. For notational simplicity we shall hereon write $P(\alpha)$ instead of $P(\alpha|G)$. Note that G is fully specified by the m_i's and is not a result of the theory. In the next subsection the m_i's and the packing constraints are written explicitly for three geometries corresponding to planar bilayers, curved monolayers, and inverted cylinders in the hexagonal phase.

The spd that minimizes A_c in eq 3 subject to the packing constraints of eq 4 is given by[8,10]

$$P(\alpha) = \frac{1}{y} \exp[-\beta\epsilon(\alpha) - \beta\sum_{i=1}^{L}\pi_i\phi_i(\alpha)] \qquad (5)$$

where y is the normalization constant (partition function), which is closely related, though not identical,[8] to the configurational integral Z_c ($A_c = -kT\ln Z_c$; see below). The π_i are the Lagrange multipliers conjugate to the m_i, which can be evaluated by substituting $P(\alpha)$ from eq 5 into the equations of constraints (eq 4) and solving the resulting set of nonlinear equations.[8,10] The physical significance of π_i is that of a lateral pressure exerted in layer i on any given ("central") chain by its neighbors. Consistent

with this interpretation the π_i's are positive and their magnitudes increase as the packing constraints become more severe, and thus restrict conformational freedom. Maximal orientational freedom corresponds to an isolated or a "free" ("unconstrained") chain for which all $\pi_i \equiv 0$. Note that the spd given in eq 5 is a general expression valid for all the geometries. The difference between the geometries enters via the constraint equations (4) and hence through the π_i's, which depend on the m_i's.

It may be noted that an alternative (more detailed) derivation of eq 5 is possible based on expansion of the many-chain configurational integral, and on the assumption that interchain forces are dominated by hard core repulsions, with the long-range forces providing a uniform attractive background.[8] In the present derivation, which is based on the minimization of A_c, the short-range repulsive forces are accounted for by the constraint equations.

(b) Geometry and Packing Constraints. We now consider the packing constraints for the three relevant geometries: bilayers, monolayers, and cylinders in an inverse hexagonal phase. The first two cases will be briefly outlined since they have been thoroughly studied earlier, in refs 2a and 10a, respectively. The third case has not been treated before and will be considered in detail below.

(1) Planar Bilayer. For computational purposes it is convenient to divide the hydrophobic core into $2L$ parallel layers of equal width, Δl, and volumes M_i (Figure 2b). For the planar bilayer M_i = const and hence $m_i = M_i/N = m$ = const. The value of m is proportional to the area per head group, a (namely, $mL = av$ where v is the chain's volume). Some of the layers (especially near the midplane) can be reached by chains originating from either interface of the bilayer (Figure 2). This is taken into account in the requirement for uniform density in the hydrophobic core, which reads

$$\langle\hat{\phi}_i\rangle = \sum_\alpha P(\alpha)[\phi_i(\alpha) + \phi_{2L-i+1}(\alpha)] = m \qquad i = 1, ..., 2L \qquad (6)$$

where $\phi_i(\alpha)$ is the volume that a chain in conformation α occupies in layer i. The two terms in eq 6 represent the contribution to the packing constraint from chains in conformation α originating from the two opposite interfaces.[2a] Thus, $\langle\hat{\phi}_i\rangle = \langle\phi_i\rangle + \langle\phi_{2L-i+1}\rangle$, is the average volume per chain in layer i, with the average taken over chains from both interfaces.

(2) Monolayer. In a monolayer, unlike "compact" aggregates like bilayers or micelles, the chains need not fill all the volume available to them. Thus, instead of the equality constraints of eq 4 or eq 6, we now have the following inequalities:

$$\langle\phi_i(\alpha)\rangle \leq m_i \qquad (7)$$

The derivation of the $P(\alpha)$, which minimizes A_c subject to eq 7, is similar to the case of equality constraints, eq 4. It can be shown that for those layers i, for which the optimal $P(\alpha)$ implies $\langle\phi_i\rangle = m_i$, the lateral pressure is positive $\pi_i > 0$. On the other hand if $\langle\phi_i\rangle < m_i$, then $\pi_i = 0$, implying that the packing constraint in layer i is trivially satisfied and is thus an "irrelevant constraint".

(3) Hexagonal Phase. One important feature of the previous two cases is that in both bilayers and monolayers all chains have the same local environment, or in other words, all chains are equivalent. Here we face a situation where a given region can be reached by chains originating from three different cylinders. Furthermore, as is shown in Figure 1a, chains originating from different regions of the cylinder are not equivalent. Thus, the symmetry of this geometry is lower than in the former cases, and consequently, the packing constraints are more complicated. To calculate $P(\alpha)$ for the hexagonal phase we can again divide the hydrophobic region into layers. However, because of the lower symmetry, there is more than one way of doing so. We found that the most convenient division is the one described in Figure 1b. Basically this scheme corresponds to prescribing a set of concentric cylindrical shells around each cylinder. In the hexagonal phase, overlap exists between shells corresponding to neighboring cylinders. Since some points in the hydrophobic region can be reached by chains originating from two (or more) adjacent cylinders, this overlap must be taken into account in formulating the packing constraints. That is, the constraints should reflect

---

(14) Flory, P. J. *Statistical Mechanics of Chain Molecules*; Wiley-Interscience: New York, 1969.

the fact that the volume (m_i) of layer i around a specific cylinder, say cylinder I in Figure 1b, is partially filled by chains originating from cylinders K and J. Thus, clearly, $\langle \phi_i \rangle$, the average volume taken up by a chain originating from cylinder I in layer i around this cylinder, is less than m_i. Formally this fact can be expressed as

$$\langle \phi_i \rangle = m_i[1 - \sum_{j,k=1}^{L} K_{ijk}f_{ijk}] \qquad i = 1, ..., L \qquad (8)$$

with the factor in brackets correcting for the overlap between different cylinders. The subscripts i,j,k in eq 8 designate layers around cylinders I, J, and K, respectively. The upper limit L corresponds to the most distant layer that can be reached by a (fully extended) chain originating from cylinder I. f_{ijk} denotes the (volume) fraction of m_i that overlaps with layers j and k of the other cylinders, and K_{ijk} stands for the fraction of the overlap volume that is filled up by chains originating from cylinders J and K.

In most relevant cases, and in all the calculations presented in section 3, the distance between the interfaces of two neighboring cylinders ($2l_1$ in Figure 1) is smaller than the length, l_c, of the fully extended amphiphile chain. Furthermore, $l_c \gtrsim l_2$; i.e., the chain is just slightly longer than the minimal distance between the midpoint of three neighboring cylinders to the interface of any of these cylinders. (Clearly, l_c must exceed l_2 to avoid "holes" between the cylinders. On the other hand, from volume filling requirements it follows that l_c cannot significantly exceed l_2, since this would imply unreasonably large head-group areas a.) Thus, the volume between cylinders (see Figure 1b) involves three types of regions corresponding to (i) overlap between three cylinders, (ii) overlap between two cylinders, and (iii) no overlap. In terms of the layer numbers i,j,k, the three regions correspond respectively to (i) $i \simeq j \simeq k$ (i.e., the central region), (ii) e.g., $i \simeq j$ and $k \sim 1$ (overlap between cylinders I and J. "$k \sim 1$" means an "inner" layer close to cylinder K), and (iii) i "considerably larger" than both j and k, (e.g., $i = 5$ and $j = k = 1$ in Figure 1b).

The f_{ijk}'s are geometrical quantitites dictated by the two geometrical characteristics of the H_{II} phase (e.g., R and l_2) and by the choice of the "computational parameter" L (or Δl). On the other hand the K_{ijk}'s are more complex quantities, which are not constant but, rather, functions of the $\langle \phi_i \rangle$'s. To clarify this point let us consider the simpler case of a planar bilayer. The bilayer's analog of eq 8 is

$$\langle \phi_i \rangle = m_i[1 - \sum_{i,j}^{2L} K_{ij}f_{ij}] \qquad i = 1, ..., 2L \qquad (9)$$

with i and j denoting the layers corresponding to the two bilayer's interfaces I and J (see Figure 2b). If, as in Figure 2b, the two sets of layers fully overlap, we have $f_{ij} = 1$ for $j = j^* = 2L - i + 1$ and $f_{ij} = 0$ otherwise. The volume fraction of layer i (relative to I, and hence layer j^* relative to J), which is filled up by chains from the opposite interface (J), is

$$K_{ij}^* = \frac{\langle \phi_j^*(\alpha) \rangle}{\langle \phi_i(\alpha) \rangle + \langle \phi_j^*(\alpha) \rangle} = \frac{\langle \phi_j^*(\alpha) \rangle}{M} \qquad (10)$$

which, upon substitution into eq 9, yields eq 6, as expected.

Equation 6 can be extended to the more complex case of hexagonally arranged cylinders, thus expressing K_{ijk} in terms of the $\langle \phi_i \rangle$'s. Upon substitution into eq 8 we then obtain a set of equations for the $\langle \phi_i \rangle$'s that can be solved numerically by an iterative ("self-consistent") procedure. It turns out however that for the cases of interest here, for which numerical results are reported in section 3, a simpler choice of the K_{ijk}'s yields essentially identical results. More explicitly, we found that the extent of chain overlap ("interdigitation") is rather small and does not significantly affect the conformational properties of the chains. In other words, the chains in the hexagonal phase are not very different from those grafted (as a "monolayer") around a single cylinder. The most significant distortion of the chains in the H_{II} phase, as compared to a monolayer, is associated with the stretching of the few chains reaching the middle regions between cylinders. Based on these

notions, we found that the following (approximate) choice for K_{ijk}

$$\begin{aligned} K_{ijk} &= \tfrac{1}{3} & i &= j = k \\ &= \tfrac{1}{2} & i &= j > k \text{ or } i = k > j \\ &= 1 & i &> j, k \end{aligned} \qquad (11)$$

gives results similar to those obtained with the more detailed procedures mentioned above.

(c) Conformational Statistics. The π_i's and hence $P(\alpha)$ are obtained by numerical solution of eq 8, (see section 3 for more details). Using $P(\alpha)$, we can calculate various chain conformational properties. Of particular interest are the C–D bond order parameters, which can be measured by deuterium NMR spectrometry. The order parameter of the nth (C$_n$–D) bond is defined by

$$\bar{S}_n = \langle P_2(\cos \theta_n) \rangle = \sum_\alpha P(\alpha)[3 \cos^2 \theta_n(\alpha) - 1]/2 \qquad (12)$$

where $P_2(x) = (3x^2 - 1)/2$ is the second Legendre polynomial. $\theta_n(\alpha)$ is the angle between the C$_n$–D bond and the local normal to the hydrocarbon–water interface, for a chain in conformation α. Note that in the limit of a fully extended (all-trans) chain perpendicular to the interface $\bar{S}_n = -1/2$. On the other hand, for a random distribution of bond angles $\bar{S}_n = 0$. It should also be noted that the C$_n$–D bond order parameters are related to the "skeletal" order parameters S_n, corresponding to the vectors connecting carbons C$_{n-1}$ and C$_{n+1}$ of the chain, via $S_n = -2\bar{S}_n$. Thus, for a fully extended chain perpendiculary oriented with respect to the interface, $S_n = 1$ for all n, whereas for a random distribution, $S_n = 0$.

The free energy per molecule, in the mean field approximation, can be calculated by substituting eq 5 into eq 3, yielding

$$A_c = -kT \ln y - \sum_{i=1}^{L} \pi_i m_i \qquad (13)$$

Recall, however, that A_c is only the chain contribution to the amphiphile's free energy. The full free energy should include the head-group term A_h. In this paper we adopt for A_h a simple phenomenological form, based on the familiar model of the "opposing forces".[12,13] These "forces" include the effective attraction between head groups arising from the hydrophobic effect, which tends to minimize the contact area between the water and the alkyl chains. This tendency is opposed by excluded volume or electrostatic (ionic, dipole–dipole) repulsions between the head groups, which tend to increase the area per molecule. The first contribution to the free energy is usually modeled by a "surface tension" term γa, while the second is assumed to be (approximately) inversely proportional to a. This yields

$$A_h = \gamma[a - a_0^2/a] \qquad (14)$$

where γ is the effective interfacial tension and a_0 is the head-group area that minimizes A_h.

For curved interfaces, this expression is often replaced by the modified phenomenological form[13]

$$A_h = \gamma[a - a_0^2/a(1 + D/R)] \qquad (15)$$

Here $1/R = 1/R_1 + 1/R_2$, with R_1 and R_2 denoting the principal radii of curvature of the hydrocarbon–water interface and D a parameter of the model (an effective distance between the head groups and the neutral surface). Adding the head-group free energy A_h to the tail free energy A_c, one can calculate $A = A_c + A_h$ for various aggregation geometries G. The geometry is determined completely by the area per head group a and by the radii of curvature R_1 and R_2. (It is straightforward to show that the m_i's are simply related to these quantities.)

Amphiphiles packed in a lamellar phase depend on a single geometric parameter, namely, the bilayer thickness d_l or the area per head group a (Figure 2a). These two parameters are related via $a = v/d_l$, where v is the chain's volume.

Two geometrical parameters suffice to characterize the H_{II} phase (Figure 1b): the radius of the water cylinders (R) and the distance between two cylinder centers (d). All other geometrical
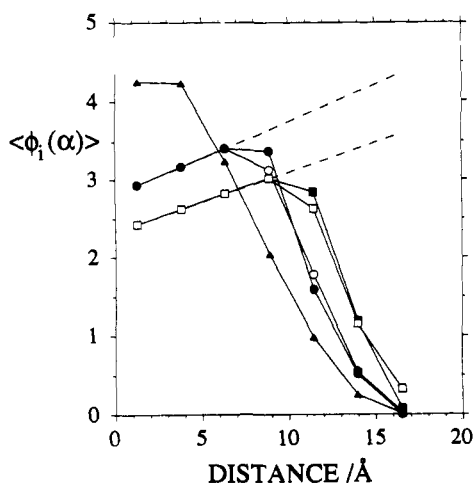
Figure 3. Chain segment density in the H_{II} phase. The figure shows the average number of chain segments in layer i around cylinder I; for chains originating from this cylinder, see Figure 1. (The distance scale corresponds to the distance from the interface of cylinder I to the middle of layer i; namely, to $(i = \frac{1}{2})\Delta l$ with $i = 1, 2, ...$ and $\Delta l = 2.51$ Å. The ϕ_i are normalized according to $\sum\phi_i = n = 15$, the number of chain segments.) All the results here are for cylinders of radius $R = 30$ Å. ▲, free chain. ■ and ●, chains in the H_{II} phase, with the area per head group $a = 24.8$ and 29.9 Å², respectively. The symbols □ and ○ correspond to chains grafted on a single cylinder (i.e., monolayer) at the same area per head group as the corresponding solid symbols. The dashed lines describe m_i, the volume (per chain) in layer i.

characteristics can be expressed in terms of these parameters; e.g., $l_1 = (d/2) - R$ and $l_2 = (l_1 + R)/\cos(\pi/6) - R \simeq 1.15(l_1 + R) - R$ (Figure 1a). Similarly, the area per head group is given by $a = 4Rv/(3^{1/2}/\pi d^2 - 2R^2)$.

3. Results and Discussion

All the calculations presented here were carried out for 14-carbon chains, i.e., $H(CH_2)_{13}CH_3$ amphiphiles, with H denoting the (structureless) head group. We have used $T = 300$ K and a gauche energy $\epsilon_g = 500$ cal/mol. The chains are represented by the rotational isomeric state model.[14] Chain conformations are generated as follows:[10a] first *all* the bond sequences are generated according to the RIS model (each C–C bond has three possible states: t = trans, g^+ = gauche$^+$ and g^- = gauche$^-$). Then we randomly sample three head-group positions for each of the bond sequences (within a small interval of ~1.5 Å around the interface). Finally, we randomly sample 12 overall orientations for each bond sequence and head-group position; thus every bond sequence is sampled 36 times.

In the process of generating chain conformations, we discard all overlapping ("self-avoiding") sequences. Furthermore, we keep only those conformations in which all segments are confined to the hydrophobic region. Thus the number of acceptable conformations depends on the curvature of the interface. (This number is higher in the inverse hexagonal phase as compared to the planar bilayer.) For each chain conformation generated we calculate $\phi_i(\alpha)$ and all other conformational properties of interest, e.g., $P_2(\cos\theta(\alpha))$. The $\phi_i(\alpha)$'s are then used in the equations of constraints to solve for the π_i's and hence for $P(\alpha)$.

In the calculations presented here conformations are separately generated for the planar bilayers of the L_α phase, and for the inverse cylindrical geometry with $R = 25$ Å and $R = 30$ Å of the H_{II} phase.

(a) Conformational Properties. Figure 3 shows the spatial distribution of chain segments for the H_{II} phase. More precisely, for chains anchored to cylinder I, the figure shows $\langle\phi_i\rangle$, the average number (or volume) of chain segments in layer i (i.e., at the interval $i\Delta l - (i - 1)\Delta l$), as a function of the distance $i\Delta l$ from the interface of cylinder I. The geometrical parameters chosen are $R = 30$ Å and $l_2 = 17.7$ Å or $l_2 = 15.5$ Å. The corresponding areas per head group are $a = 24.8$ Å² and $a = 29.9$ Å², respectively. For comparison, we also show (i) the segment distribution

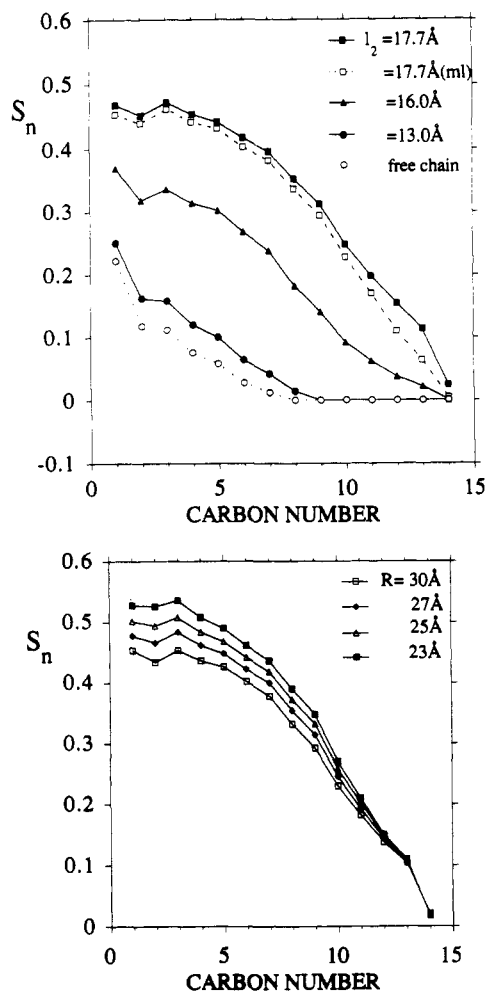**Figure 4.** (a, top) Bond order parameters in the H_{II} phase ($S_n = -2\tilde{S}_n$, where $\tilde{S}_n$ is the P_2 order parameter of the nth C–D bond). All the results are for cylinders of radius $R = 30$ Å. The areas per head group corresponding to the three l_2 values (see Figure 1) are $a = 38.6, 28.6,$ and 24.8 Å², for $l_2 = 13.0, 16,$ and 17.7 Å, respectively. The open symbols correspond to monolayers (ml). (b, bottom) Bond order parameter profiles for different cylinder radii and fixed l_2.

for chains anchored to a single cylinder (monolayer) at the same area per head group and (ii) the segment distribution of a single chain on a cylinder (i.e., unconstrained free chain).

As expected, the chains are farther stretched as the area per chain a is decreased, or equivalently, as l_2 is increased. (Recall that there is no restriction on a for a free chain. The free chain determines its own lateral dimension, so as to minimize its conformational free energy.) Note the close similarity between chains packed in the hexagonal phase and those anchored, as a monolayer, around a single cylinder. This indicates that chain interdigitation in the overlap region (see Figures 1 and 2) is associated with negligible perturbations in chain conformational properties. The straight dashed lines in Figure 3 show m_i, the volume per chain in layer i, as a function of the distance $i\Delta l$ from the cylinder's interface. (m_i varies linearly with the distance, $m_i = m_1[(i - 1/2)/R + 2R/\Delta l]$ with m_1, the volume of the innermost layer, being proportional to the area per head group.) Thus $\langle\phi_i\rangle/m_i$ is the volume fraction of the ith layer around cylinder I, which is filled up by chains originating in cylinder I. From the figure it is clear that the range over which $\langle\phi_i\rangle/m_i \sim 1$ increases as a decreases.

The next set of results is for the C–D bond order parameter. We shall first show how the order parameters depend on the radii of the cylinders and the distance between them. Then we shall compare the calculated order parameters with the corresponding values for the L_α phase and finally compare them with experimental data. In Figure 4a we show the bond order parameters S_n for chains in the H_{II} phase for different values of the thickness
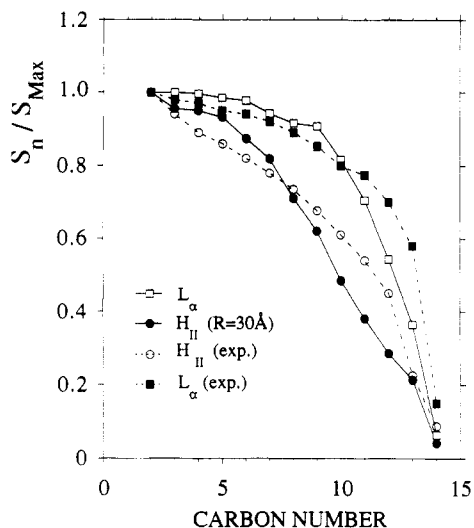
Figure 5. Bond order parameter profiles in the H_{II} phase and in the L_α phase. The calculated results are for $a = 26.6$ $Å^2$ (for both phases). Also shown are the experimental results of Sternin et al.[5]

of the hydrocarbon region l_2, keeping the cylinder radius constant, $R = 30$ Å. (Recall that $S_n = -2\tilde{S}_n$.) We note a continuous decrease of the order parameters down the chain, from the head group to the terminal segment. Note also that the magnitude of the order parameters increases as l_2 increases (a decreases), since the chains need to stretch further in order to reach the inner regions. For small l_2 values, e.g., $l_2 = 13$ Å ($a = 38.6$ $Å^2$), the packing constraints are not significant and the chains resemble free chains.

Similar trends are displayed in Figure 4b, which shows how the order parameter profile varies with the cylinder radius R, for a given hydrophobic core thickness l_2. From the relations between l_2, R, and a ($a = 4Rv/[3(3)^{1/2}/\pi(R + l_2)^2 - 2R^2)]$ it follows that, for a fixed l_2, a decreases as R decreases, explaining the increase in S_n as R decreases.

Figure 5 shows the order parameter profiles of the chains in the H_{II} phase and in the L_α phase, i.e., in a planar bilayer. In all cases the area per head group is $a = 26.6$ $Å^2$. The H_{II} phase allows more conformational freedom than the L_α phase, as indicated by the faster decline of S_n with n. The typical plateau in S_n of planar bilayers is replaced by a monotonic decrease in the hexagonal phase, due to "milder" packing constraints in the H_{II} phase. (m_i is a constant for the planar bilayer and increases linearly in H_{II}.)

Figure 5 shows also the experimental results of Sternin et al.,[3] who measured the order parameters in the L_α and H_{II} phases using a mixture of 1-palmitoyl-2-oleylphosphatidylethanolamine and perdeuterated tetradecanol in water. These authors did not report the values of R or a. The value of a (26.6 $Å^2$) was chosen to give good agreement with the experiments. While the agreement may not be perfect, we consider it very satisfactory in view of the complexity of the system.

(b) Thermodynamics. In Figure 6 the energy, entropy, and free energy of the chains in the H_{II} phase are shown as a function of l_2. Figure 6a reveals that the internal chain energy E_c (which is proportional to the average number of gauche bonds) decreases as l_2 increases and as R decreases. This is consistent with the fact that the extent of chain stretching increases with l_2, i.e., with intercylinder separation. As noted already with regard to Figure 1, the behavior of the chains in the H_{II} phase is quite similar to that of chains anchored to a single cylinder (monolayer).

As expected, the entropy S_c decreases with l_2, reflecting the substantial loss of conformational freedom upon chain stretching (Figure 6b). The decrease of E_c with chain stretching lowers the conformational free energy A_c, whereas the corresponding decrease in S implies an increase in A_c. Quantitatively, the decrease in S_c is stronger and will thus dominate A_c, as shown in Figure 6c. The minimum of A_c at $l_2 = 13$ Å, corresponds to a free chain (i.e., no packing constraints).
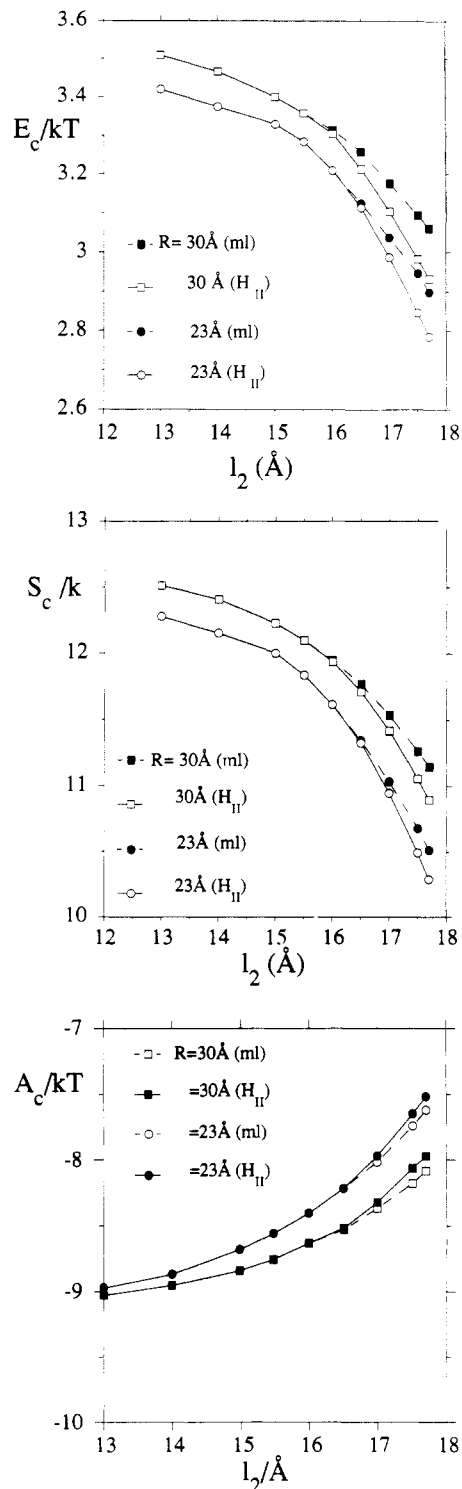

Figure 6. (a, top) Average conformational energy per chain in the H_{II} phase as a function of l_2, which measures the distance between adjacent cylinders (see Figure 1), for two values of the cylinders radii R. (ml corresponds to monolayer.) (b, middle) Conformational entropy per chain in the H_{II} as a function of l_2. (c, bottom) Conformational free energy per chain in the H_{II} $A_c = E_c - TS_c$, as a function of l_2 ($T = 300$ K).

Figure 7 shows the chain's free energy in the hexagonal and in the lamellar phases as a function of the area per head group. Because of the larger conformational freedom in the hexagonal phase it is more favorable for all values of a. Thus, a crossover in stability from one geometry to another, i.e., a transition from the L_α to the H_{II} phase at some value of a, must involve additional contributions to the total free energy. Interaggregate (cylinders or bilayers) interactions is one major contribution to the system's free energy that must be considered. Another important free
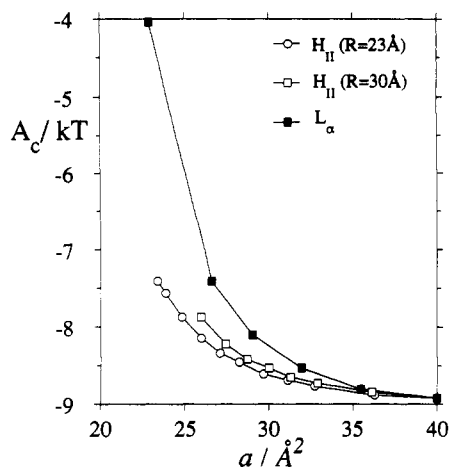
Figure 7. Conformational free energy per chain in the H_{II} and L_α phases as a function of the area per head group.
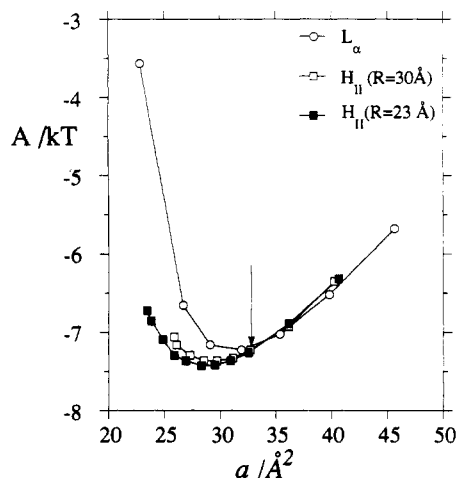

Figure 8. Average free energy per chain (including both head-group and chain contributions), as a function of the area per head group, in the H_{II} and the L_α phases.

energy term is the head-group contribution A_h. In the following we briefly consider the combined effect of A_c and A_h on the relative stability of the two phases.

We have calculated $A = A_c + A_h$, using the mean field theory for A_c and the phenomenological expressions, eqs 14 and 15, for

A_h. From eq 15 it is clear that, for the same value of a, A_h will be larger for the H_{II} phase ($R > 0$) than for the L_α ($R = \infty$) phase, reflecting the stronger head-group repulsion for convex hydrocarbon–water interfaces. On the other hand, $A_c(a)$ is higher for the L_α phase because of the more stringent packing constraints. As a numerical example, Figure 8 shows $A = A_c + A_h$ vs a for $\gamma = 0.1kT$, $D = 2.5$ Å and $a_0 = 20$ Å^2. We see that the hexagonal phase is more stable for head-group areas lower than a certain "critical" area a^* ($\sim$34 Å^2 for the parameters chosen), whereas above a^* the lamellar phase is the one with lower free energy. Clearly, for other choices of molecular parameters for crossover from H_{II} to L_α symmetry will take place at different values of a^*. Our main purpose here was to demonstrate that such a transition is indeed possible.

The qualitative trends implied by the results above are consistent with the experimental observation of a phase transition from the L_α to the H_{II} phase upon decreasing the water content in the system.[1a,6,15] This is because a decrease in water concentration is equivalent to a decrease in the average area per head group.

4. Concluding Remarks

In this paper we have analyzed a number of conformational and thermodynamic properties of amphiphilic molecules packed in the inverse hexagonal phase H_{II}. It was found that for the same area per molecule the degree of chain conformational freedom in the hexagonal phase (H_{II}) is higher than in the lamellar (L_α) phase and is comparable to that in a cylindrical monolayer of grafted chains. The last finding indicates that chain overlap (interdigitation) in the H_{II} phase does not significantly affect the conformational freedom of the chains. By a thermodynamic analysis based on a free energy expression that takes into account both tail and head-group contributions, it was found that a crossover from the H_{II} to the L_α phase may take place as the area per head group exceeds a certain critical value a^*.

(15) Luzzati, V. In *Biological Membranes*; Chapmann, D., Ed.; Academic Press: New York, 1968; Vol. 1.